Theoretical force-field model for blue-shifted hydrogen bonds with fluoromethanes. Chem Phys

ARTICLE *in* CHEMICAL PHYSICS · OCTOBER 2006

Impact Factor: 1.65 · DOI: 10.1016/j.chemphys.2006.06.007

2 AUTHORS:

Eugene S Kryachko
University of Liège
139 PUBLICATIONS **2,031** CITATIONS
SEE PROFILE

Alfred Karpfen
University of Vienna
162 PUBLICATIONS **4,284** CITATIONS
SEE PROFILE

Available online at www.sciencedirect.com
SCIENCE DIRECT®
Chemical Physics xxx (2006) xxx–xxx
Chemical Physics
www.elsevier.com/locate/chemphys

Theoretical force-field model for blue-shifted hydrogen bonds with fluoromethanes

Eugene S. Kryachko [a,b,*], Alfred Karpfen [c,*]

[a] Department of Chemistry, Bat. B6c, University of Liege, Sart-Tilman, B-4000 Liege 1, Belgium
[b] Bogoliubov Institute for Theoretical Physics, Kiev 03143, Ukraine
[c] Institute for Theoretical Chemistry, University of Vienna, Währinger Straße 17, A-1090 Vienna, Austria

Received 4 April 2006; accepted 8 June 2006

Abstract

It is demonstrated that the contraction of the C–H bonds of fluoromethanes in some subclass of blue-shifting complexes and the concomitant blue shifts of their stretching vibrational modes are a direct consequence of the intramolecular mode coupling between C–H and C–F bonds. This subclass of the so-called blue-shifted complexes includes those blue-shifting complexes, where the C–F bond of fluoromethanes participates in the pre-formation of the dominating C–F···H–Y halogen–hydrogen bond with the conventional proton-donor molecule Y–H. The formation of the latter elongates this 'spectator' C–F bond that in turn causes the C–H bond(s) of fluoromethanes to contract. It is therefore an intrinsic, intramolecular feature of the fluoromethanes that underlies the phenomenon of an 'intramolecular negative response'. This phenomenon is a key mechanism of a blue shift of this subclass of blue-shifted complexes. To understand the origin of the intrinsic intramolecular negative response of the fluoromethanes, a physical and analytically solvable model of the intramolecular mode coupling that is mainly based on the harmonic force field ansatz is proposed. It is explicitly shown that this model fairly agrees with the calculated contractions of the C–H bonds in the fluoromethanes–hydrogen fluoride complexes $CH_nF_{4-n}\cdot\cdot\cdot(HF)_{1\leqslant m\leqslant 4}$ ($1\leqslant n\leqslant 3$). The model concludes that it is the intramolecular mode coupling patterns of the fluoromethanes that entail their intrinsic negative response. The related enigmatic nature of the formation of the complexes $CHF_3\cdot\cdot\cdot OH_2$ and $CHF_3\cdot\cdot\cdot NH_3$ is revisited invoking particularly the traditional approach of embedding the studied system into an external homogeneous electric field.

Keywords: Hydrogen bonding; Blue-shifted hydrogen bond; Harmonic force-field model; Anharmonic corrections; Multimode Hamiltonian; Linear intermode coupling; Intramolecular negative response

1. Prelude

It is nearly half a decade that blue-shifting hydrogen bonds of the type C–H···X are an exceptional theme of many researchers worldwide [1–3]. Such key features as the contraction of the C–H bond, the concomitant blue shift of the stretching vibrational mode ν(C–H) and the decrease of its infrared intensity, and also the absence of a direct relationship that links the hydrogen bonding interaction energy to the magnitude of the blue shift unequivocally place them in a sharp contrast with the classical, conventional hydrogen (H–) bonds [4–10] and raise the question of what is actually their place in the theory of molecular interactions [1–3].

* Corresponding authors. Address: Department of Chemistry, Bat. B6c, University of Liege, Sart-Tilman, B-4000 Liege 1, Belgium. Fax: +32 4 366 3413 (E.S. Kryachko), fax: +43 1 4277 9527 (A. Karpfen).
E-mail addresses: eugene.kryachko@ulg.ac.be (E.S. Kryachko), alfred.karpfen@univie.ac.at (A. Karpfen).

0301-0104/$ - see front matter © 2006 Published by Elsevier B.V.
doi:10.1016/j.chemphys.2006.06.007

Two major avenues can be traced in the studies of blue-shifting hydrogen bonds. One avenue aims to answer the question of whether the class of blue-shifting H-bonds is exceptional and includes only few representatives, or whether it can be extended, either by experimental or theoretical means, to a larger variety of complexes that unveil larger blue shifts, comparable to the red shifts of conventional hydrogen bonds? It is indeed that avenue, where the main progress has been achieved so far in this area. Another avenue is directed to resolve the longstanding paradigm of what is the mechanism of a blue shift (see, e.g., Refs. [1–3,11–18] and references therein). Several theoretical approaches, such as the charge-transfer natural bond orbital analysis [11–13], an interplay of hyperconjugation and rehybridization [14], the energy decomposition scheme [15], repulsive (Pauli) steric interactions [16], and finally, the modeling of the formation of the C–H···X hydrogen bond via embedding into a homogeneous electric field [17–21], have been invoked to rationalize the blue-shifting mechanism.

Following the former avenue, we have recently extended the class of blue-shifting hydrogen bonds by including the fluoromethanes–hydrogen fluoride complexes $CH_nF_{4-n}\cdots(HF)_m$ ($1 \leqslant n \leqslant 3$; $1 \leqslant m \leqslant 3$) [22,23] which exhibit rather large calculated C–H blue shifts that fall into the range of 50–60 cm^{-1} for $m = 3$. Attempting to shed light on the nature of these large blue shifts, we have partly stepped aside, toward the second avenue, and revealed that the structures of these novel blue-shifting hydrogen-bonded complexes, sketched in Tables 1 and 2, definitely imply that the contraction of their C–H bond(s) mostly originates from the intrinsic, intramolecular nature of fluoromethanes themselves, namely from a specific intramolecular mode coupling – precisely, it is caused by the elongation of the C–F bond while it participates in the formation of the (C)F···H–F halogen–hydrogen bond. Other blue-shifting hydrogen-bonded complexes, also formed between $(HF)_n$ clusters and alternative X–F proton donors, such as fluorophosphines, fluoroarsines [21] and fluorosilanes [24] (X = Si, P, and As), showed the existence of a similar intramolecular coupling between X–H and X–F bonds. This idea

Table 1
Selected properties of the complexes $CH_nF_{4-n}\cdots HF$ ($1 \leqslant n \leqslant 3$)

I_1. F_3C-H···FH 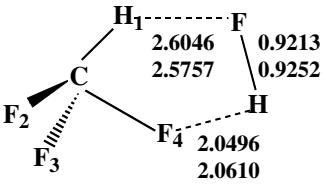 	MP2/6-311++G(2d,2p) [23] (upper entry): $\Delta R(C–H_1) = -0.0007$ Å $\Delta\nu(C–H_1) = 16$ cm^{-1} $\Delta A(C–H_1) = -15$ km mol^{-1} $\Delta E = -3.3$ kcal mol^{-1} $\Delta E_{BSSE} = -2.2$ kcal mol^{-1} $\Delta R(C–F_4) = 0.0172$ Å $\Delta R(C–F_{2,3}) = -0.0050$ Å MP2/aug-cc-pVTZ [23] (lower entry): $\Delta R(C–H_1) = -0.0007$ Å $\Delta\nu(C–H_1) = 15$ cm^{-1} $\Delta A(C–H_1) = -14$ km mol^{-1} $\Delta E = -3.1$ kcal mol^{-1} $\Delta E_{BSSE} = -2.5$ kcal mol^{-1} $\Delta R(C–F_4) = 0.0164$ Å $\Delta R(C–F_{2,3}) = -0.0046$ Å
II_1. CH_2F_2···HF 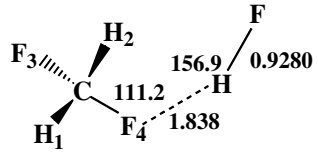 	MP2/aug-cc-pVTZ [22]: $\Delta R(C–H_1) = -0.0014$ Å $\Delta R(C–H_2) = -0.0007$ Å $\Delta\nu(C–H) = 13, 20$ cm^{-1} $\Delta A(C–H) = -13, -12$ km mol^{-1} $\Delta E = -4.3$ kcal mol^{-1} $\Delta E_{BSSE} = -3.7$ kcal mol^{-1} $\Delta R(C–F_4) = 0.0190$ Å $\Delta R(C–F_3) = -0.0085$ Å
III_1. CH_3F···HF 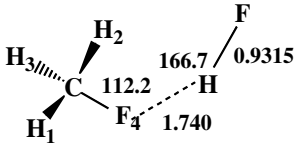 	MP2/aug-cc-pVTZ [22]: $\Delta R(C–H_{1,3}) = -0.0020$ Å $\Delta R(C–H_2) = -0.0013$ Å $\Delta\nu(C–H) = 16, 26, 29$ cm^{-1} $\Delta A(C–H) = -9, -14, -11$ km mol^{-1} $\Delta E = -6.1$ kcal mol^{-1} $\Delta E_{BSSE} = -5.5$ kcal mol^{-1} $\Delta R(C–F_4) = 0.0168$ Å

Throughout this work, A stands for IR activity, E_{BSSE} indicates the basis-set-superposition-error-corrected stabilization energy, and the frozen-core approximation of the second-order perturbation Møller–Plesset method (MP2) is assumed.

Table 2
Selected properties of blue-shifted complexes $CH_nF_{4-n}\cdots(HF)_{2\leqslant m\leqslant 3}$ $(1 \leqslant n \leqslant 3)$

I_2. $CHF_3\cdots(HF)_2$

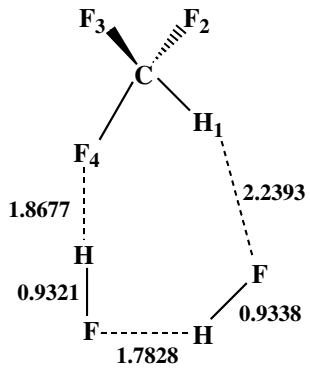

MP2/aug-cc-pVTZ [23]:
$\Delta R(C–H_1) = -0.0012$ Å
$\Delta \nu(C–H_1) = 30$ cm^{-1}
$\Delta A(C–H_1) = -20$ km mol^{-1}
$\Delta E = -10.9$ kcal mol^{-1}
$\Delta E_{BSSE} = -9.4$ kcal mol^{-1}
$\Delta R(C–F_4) = 0.0303$ Å
$\Delta R(C–F_{2,3}) = -0.0076$ Å

I_3. $CHF_3\cdots(HF)_3$

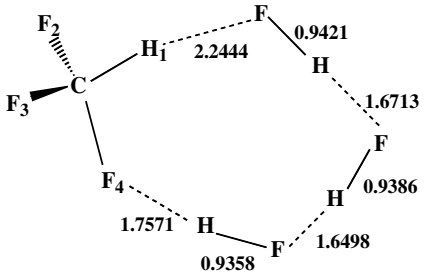

MP2/aug-cc-pVTZ [23]:
$\Delta R(C–H_1) = -0.0039$ Å
$\Delta \nu(C–H_1) = 60$ cm^{-1}
$\Delta A(C–H_1) = -19$ km mol^{-1}
$\Delta E = -20.1$ kcal mol^{-1}
$\Delta E_{BSSE} = -17.5$ kcal mol^{-1}
$\Delta R(C–F_4) = 0.0318$ Å
$\Delta R(C–F_{2,3}) = -0.0074$ Å

II_2. $CH_2F_2\cdots(HF)_2$

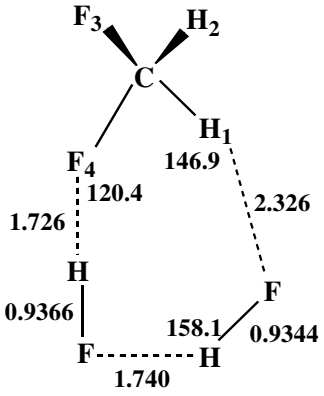

MP2/aug-cc-pVTZ [22]:
$\Delta R(C–H_1) = -0.0019$ Å
$\Delta R(C–H_2) = -0.0020$ Å
$\Delta \nu(C–H) = 24,\ 38$ cm^{-1}
$\Delta A(C–H) = -13,\ -21$ km mol^{-1}
$\Delta E = -7.7$ kcal mol^{-1}
$\Delta E_{BSSE} = -6.7$ kcal mol^{-1}
$\Delta R(C–F_4) = 0.0304$ Å
$\Delta R(C–F_3) = -0.0100$ Å

II_3. $CH_2F_2\cdots(HF)_3$

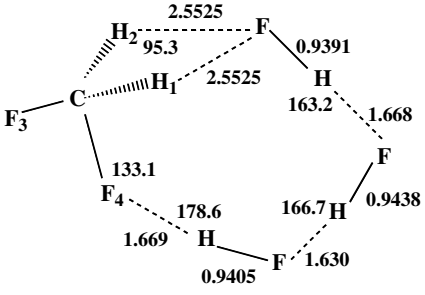

MP2/aug-cc-pVTZ [22]:
$\Delta R(C–H_1) = -0.0038$ Å
$\Delta R(C–H_2) = -0.0038$ Å
$\Delta \nu(C–H) = 43,\ 58$ cm^{-1}
$\Delta A(C–H) = -23,\ -16$ km mol^{-1}
$\Delta E = -6.3$ kcal mol^{-1}
$\Delta E_{BSSE} = -5.2$ kcal mol^{-1}
$\Delta R(C–F_4) = 0.0333$ Å
$\Delta R(C–F_3) = -0.0113$ Å

(*continued on next page*)

Table 2 (*continued*)

III$_2$. $CH_3F\cdots(HF)_2$ 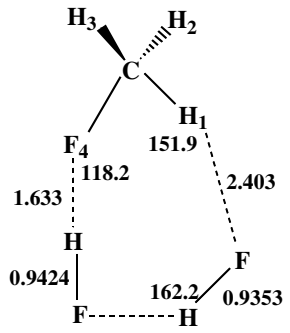	MP2/aug-cc-pVTZ [22]: $\Delta R(C–H_1) = -0.0020$ Å $\Delta R(C–H_{2,3}) = -0.0027$ Å $\Delta\nu(C–H) = 22, 39, 40\ cm^{-1}$ $\Delta A(C–H) = -6, -13, -22\ km\ mol^{-1}$ $\Delta E = -9.8\ kcal\ mol^{-1}$ $\Delta E_{BSSE} = -8.8\ kcal\ mol^{-1}$ $\Delta R(C–F_4) = 0.0278$ Å
III$_3$. $CH_3F\cdots(HF)_3$ 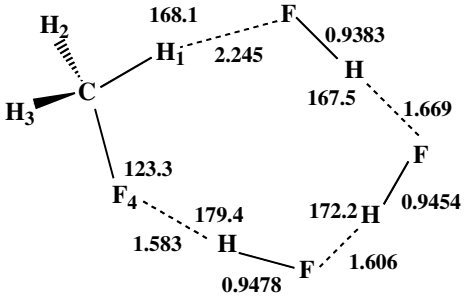	MP2/aug-cc-pVTZ [22]: $\Delta R(C–H_1) = -0.0028$ Å $\Delta R(C–H_2) = -0.0026$ Å $\Delta R(C–H_3) = -0.0032$ Å $\Delta\nu(C–H) = 26, 42, 52\ cm^{-1}$ $\Delta A(C–H) = 0, -14, -20\ km\ mol^{-1}$ $\Delta E = -8.1\ kcal\ mol^{-1}$ $\Delta E_{BSSE} = -7.0\ kcal\ mol^{-1}$ $\Delta R(C–F_4) = 0.0321$ Å

has allowed to recently predict new blue-shifting complexes between formaldehyde and hydrogen fluoride clusters with large blue shifts reaching 100 cm^{-1} [20].

Table 1, in our opinion, is a doorway to understand the idea which underlies large blue shifts in the aforementioned subclass of complexes and to develop a theoretical and analytically solvable model that constitutes a chief goal of the present work. Let us begin with considering the dimeric systems, **II**$_1$: $CH_2F_2\cdots HF$ and **III**$_1$: $CH_3F\cdots HF$ which do not actually belong to the blue-shifting complexes, rather to the complexes with a single conventional C–$F_4\cdots$H–F halogen–hydrogen bond [22] (see also footnote 3 therein). Their global-minimum structures are *open* since the "closure" C–H$\cdots$F contacts are not formed. The C–F_4 bond of CH_2F_2 or CH_3F acts as a typical proton acceptor and thus, according to the canons of the hydrogen bond theory [4–10], undergoes an elongation by 17–19 mÅ. This is one side of the story that we intend to tell.

Another side of this story is that the elongation of the 'spectator' C–F_4 bond in the complexes $CH_2F_2\cdots HF$ and $CH_3F\cdots HF$, caused by the formation of a conventional C–$F_4\cdots$H–A halogen–hydrogen bond, induces a contraction of the non-interacting and remote C–H bonds by 1.3–2.0 and 0.7–1.4 mÅ. The C–H stretches mirror that by shifting upward by 16–29 and 13–20 cm^{-1}, respectively. This obviously means that the entire phenomenon of the shortening of the fluoromethane C–H bonds and the concomitant blue shifts of their stretching vibrational modes in this subclass of blue-shifting complexes is merely a consequence of the elongation of the C–F_4 bond and is, hence, an *intrinsic*, *intramolecular feature* of the fluoromethanes CH_2F_2 and CH_3F which is hereafter called as an '*intramolecular negative response*' (or an '*intrinsic negative response*' (INR)). Fig. 1 illustrates the INR phenomenon for CH_2F_2 and CH_3F. In fact, this is the feature that, as we reckon, largely underlies the blue-shifting mechanism of some subclass of *blue-shifting hydrogen bonds* whose blue shifts are caused by the pre-formation of a strong and dominant conventional hydrogen bond and which are hereafter named as the *blue-shifted hydrogen bonds* [20–24]. In fact, the INR feature loosely determines a broader and the so-called INR class of molecules (INR molecules) containing X–H_i bonds that might be involved in the formation of blue-shifted hydrogen bonds, if the following necessary pre-conditions are obeyed: (i) the existence of a leading conventional hydrogen bond between a given INR molecule acting as proton acceptor via its X–A bond and a guest molecule in the non-degenerate global energetic minimum; (ii) the X–H_i bond(s) of a given molecule have the INR property with respect to a vicinal spectator X–A bond; (iii) at least one X–$H_i\cdots$guest H-bond-type contact is formed. Obviously, if the effect of an intramolecular negative response of any X–H_i bond(s) to the elongation of the X–A bond dominates in the interaction with a guest molecule, even if an X–$H_i\cdots$guest H-bond contact is formed, this X–H_i bonds undergoes a contraction.

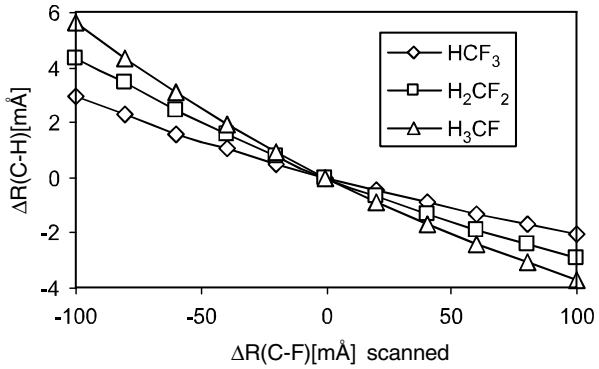

Fig. 1. MP2/aug-cc-pVTZ scans of fluoromethanes: optimized ΔR(C–H) vs. scanned ΔR(C–F).

The class of blue-shifted hydrogen bonds includes in particular the most stable cyclic complexes **II**$_2$: $CH_2F_2\cdots(HF)_2$, **II**$_3$: $CH_2F_2\cdots(HF)_3$, **III**$_2$: $CH_3F\cdots(HF)_2$, and **III**$_3$: $CH_3F\cdots(HF)_3$ gathered in Table 2. As being cyclic, they possess the dominant C–F···H–F halogen–hydrogen bonds in addition to the C–H···F–H hydrogen bonds between the fluoromethane and the $(HF)_2$ or $(HF)_3$ moieties. Compared to **II**$_1$ and **III**$_1$, a strengthening of the C–F···H–F halogen–hydrogen bond in the complexes **II**$_{2-3}$ and **III**$_{2-3}$ causes the 'spectator' C–F_4 proton acceptor bond to further elongate by ~28–32 mÅ. All C–H bonds are contracted from 1.2 to 3.9 mÅ with respect to a bare fluoromethane – those involved in the H-bond-type contact with $(HF)_2$ or $(HF)_3$ unveil H-bonded blue shifts, ranging from 22 to 58 cm^{-1}. We may therefore infer that the most important, if not even the *primary cause* of the ν(C–H) blue shifts in these complexes **II**$_{2-3}$ and **III**$_{2-3}$ is the elongation of the C–F_4 proton acceptor bond relative to that in the isolated fluoromethane as a consequence of the formation of a strong and dominant halogen–hydrogen bond. Equivalently, the latter is a dominating interaction in these complexes that determines the intramolecular rearrangement in the fluoromethanes, their bonding patterns, and their energetics. Notice in this regard that, as anticipated, the trend in the stabilization energies, −2.9, −4.3, −6.1 kcal mol^{-1}, of the three dimeric complexes $CHF_3\cdots HF$, $CH_2F_2\cdots HF$, $CH_3F\cdots HF$ fairly correlates with the equilibrium C–F bond lengths encountered in the fluoromethane monomers (1.336, 1.359, 1.388 Å) [22].

Two conjectures can therefore be drawn. The *first conjecture* states that fluoroform, CF_3H, does naturally endow the INR feature. This statement is clearly illustrated in Fig. 1 that displays the optimized C–H distances obtained from the scans of the selected R(C–F) of three fluoromethanes in the vicinity of their equilibrium structures. For all fluoromethanes, R(C–H) contracts if R(C–F) stretches. The most stable and cyclic complexes of $CHF_3\cdots F$–H (**I**$_1$), $CHF_3\cdots(HF)_2$ (**I**$_2$), and $CHF_3\cdots(HF)_3$ (**I**$_3$) having both the C–F···H–F halogen–hydrogen bonds and the C–H···F–H ones are shown in Tables 1 and 2. The formation of **I**$_1$ elongates the C–F_4 proton acceptor bond by ~16–32 mÅ whereas the non-participating C–$F_{2,3}$ bonds are contracted by ~5–8 mÅ. The C–H_1 bond is also shortened by 0.7–3.9 mÅ and its stretch undergoes a blue shift of 15–60 cm^{-1}.

The *second conjecture*, already discussed, states that the entire INR class may be treated as potential candidates to form blue-shifted complexes with the molecules which behave as conventional proton donors. Two complexes are merit to study in Section 2 to outline the limits of conjecture.

2. Interlude: complexes $CHF_3\cdots OH_2$ and $CHF_3\cdots NH_3$

These are the complexes that fluoroform forms either with water or with ammonia molecules. These complexes are fundamentally different from the viewpoint of blue-shifting hydrogen bonds: the former is usually treated as a non-conventional blue-shifting [25–32,11,13,15,16] complex, whereas the latter is, in contrast, a conventional, red-shifting H-bonded complex [32,14,16,30,34], albeit with a weak red shift. Why do these two molecules, water and ammonia, behave so strikingly different with fluoroform which however, as stated above, does belong to the INR class? We demonstrate below that their distinct behaviour originates from a subtle balance of intramolecular rearrangement dictated by the intramolecular energy surface of the INR molecule and the strength of the intermolecular interaction.

2.1. The complex $CHF_3\cdots OH_2$ Revisited

We commence with the former complex that has its own, quite remarkable story in the theory of blue-shifting hydrogen bonds [25–32,11,13,15,16]. In 1982, Paulson and Barnes [25] observed a blue shift $\Delta\nu_{exp}$(C–H) = 12 cm^{-1} for the fluoroform–water mixture in an argon matrix (an uncertainty in the assignment was mentioned in Ref. [2]). Later, in 1995, Alkorta and Maluendes [26] did not report any unusual frequency shift for this system. Four years later, Scheiner and

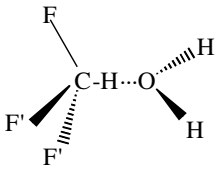

Chart 1. Structure **I** of the complex $CHF_3\cdots OH_2$.

co-workers [11] investigated this complex at the MP2/6-311+G(d,p) computational level by imposing a linear constraint on the C–H···O contact (structure **I** in Chart 1) and found a blue shift $\Delta\nu(\text{C–H}) = 42\ \text{cm}^{-1}$. A further work [13] of the quasi-linear complex **I** (Chart 1) estimated a blue shift $\Delta\nu(\text{C–H}) = 27\text{–}33\ \text{cm}^{-1}$ based on the isotope effect. The structure **I** has been pursued to study in the later works [27–31,15,16]. Interestingly, in 1964 Kaldor and Mills [32] measured the red shifts of the O–H stretching frequencies of the water molecule in the fluoroform–water complex as equal to $\Delta\nu_{\text{exp}}^{\text{sym}}(\text{O–H}) = -23\ \text{cm}^{-1}$ and $\Delta\nu_{\text{exp}}^{\text{asym}}(\text{O–H}) = -30\ \text{cm}^{-1}$.

Since the fluoroform molecule is endowed by the INR characteristic, we revisit the structure **I** of the complex $CHF_3\cdots OH_2$ in the present work via performing a limited search of its potential energy surface (PES) at the MP2(frozen core)/aug-cc-pVTZ computational level using the Gaussian suite of programs [33]. The results of this study, summarized in Fig. 2 and Table 3, are the following:

1. There exist three nearly isoenergetic stationary points **A**, **B**, and **C**. All three have C_s symmetry. The structures **A** and **B** are *open*, have an almost linear C–H···O hydrogen bond (177° and 168°), and differ in the relative orientation of the two molecules. Structure **C** is cyclic with a halogen–hydrogen bond $C_2\text{–}F_4\cdots H_8$ of 2.49 Å, comparable to the $C_2\text{–}H_1\cdots O_6$ hydrogen bond of 2.31 Å. Formally, **A** is a first-order saddle point ($\nu_{\text{TS}} = 19i\ \text{cm}^{-1}$ assigned to the intermolecular torsional mode $F\cdots OH_2$), whereas the structures **B** and **C** are minima with very low frequencies (3 and 15 cm^{-1}, respectively) for the softest intermolecular mode. Therefore, $CHF_3\cdots OH_2$ is an extraordinarily floppy molecule and its equilibrium structure is not well defined;

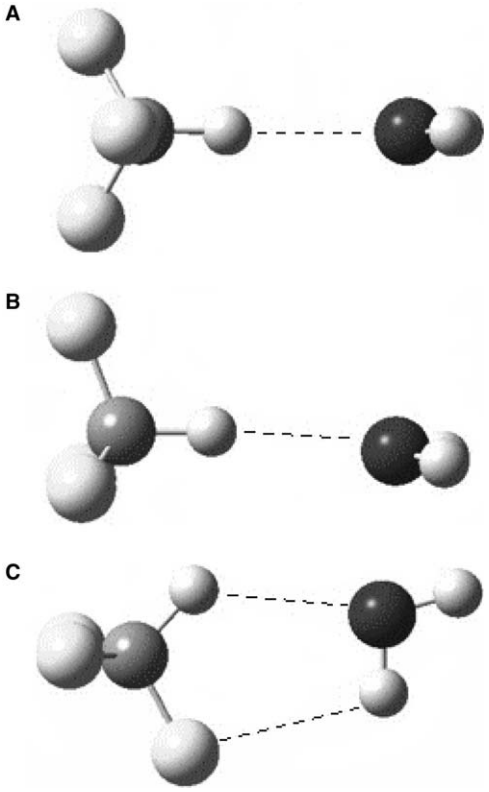

Fig. 2. MP2/aug-cc-pVTZ stationary points of the $CH_3F\cdots OH_2$ complex.

Table 3
Selected MP2/aug-cc-pVTZ properties of the structures **A**, **B**, and **C** of the $CHF_3\cdots OH_2$ complex (Fig. 2)

	A	**B**	**C**
Δr(C–H) (mÅ)	−0.9	−1.0	−2.1
$\Delta\nu$(C–H) (cm^{-1})	24	26	34
A(C–H)[a] (km mol^{-1})	4	4	4
Δr(C–F) (mÅ)	3.3, 3.8	3.3, 4.2	0.7, 8.3
$\Delta\nu$(C–F) (cm^{-1})	−9, −13, −13	−8, −13, −13	−3, −12, −15
R(CH···O) (Å)	2.21	2.21	2.31
ΔE (kcal mol^{-1})	−3.74	−3.74	−3.96
ΔE(CP)[b] (kcal mol^{-1})	−3.30	−3.30	−3.50
ΔE(CP + ZPE) (kcal mol^{-1})	−2.64	−2.62	−2.47

[a] A(C–H) of free CH_3F is equal to 22 km mol^{-1}.
[b] Counterpoise corrected.

2. Despite the three very different structures, the stationary points **A**, **B**, and **C** have much in common as far as the H-bond characteristics and other intramolecular features are concerned. In all three stationary points the C–H bond is contracted, the C–H stretching frequency is blue-shifted, and the infrared intensity of the C–H stretch is reduced. All these features are strongest in the cyclic structure **C**. The C–F bonds are stretched in **A**–**C** and their C–F stretching modes are red-shifted. In all three stationary points, the O–H stretching frequencies undergo small red shifts, from −3 to −8 cm^{-1}. Therefore, as though $CHF_3\cdots OH_2$ is a floppy system without a well-defined equilibrium structure, it definitely demonstrates the features related to the blue shifts in all three stationary points.

Let us now turn to the second complex, $CHF_3\cdots NH_3$, displayed in Chart 2.

2.2. The $CHF_3\cdots NH_3$ complex

This complex possesses C_{3v} symmetry and a perfectly linear hydrogen bond C–H···N (see also the related computational works [14,16,30,34]). The most important computational results for this complex obtained in the present work are summarized in Table 4. The calculated red shift of $\Delta\nu$(C–H) is small and equal to −16 cm^{-1}, in quite good agreement with the experimentally determined red shift of $\Delta\nu_{exp}$(C–H) = −12 cm^{-1} [30]. It is consistent with a small elongation of the C–H bond. Notice also a small reduction of the infrared intensity A(C–H) in comparison to free CHF_3. With respect to the $CHF_3\cdots OH_2$ complex, the C–F distances of $CHF_3\cdots NH_3$ are elongated and their C–F stretching frequencies are red-shifted. $CHF_3\cdots NH_3$ is characterized by a slightly higher stability compared to $CHF_3\cdots OH_2$. Indeed, the complex

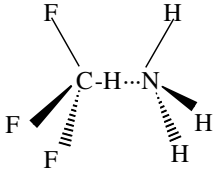

Chart 2. The global-minimum structure of the complex $CHF_3\cdots NH_3$.

Table 4
The MP2/aug-cc-pVTZ properties of the $CHF_3\cdots NH_3$ complex

Δr(C–H) (mÅ)	1.3
$\Delta\nu$(C–H) (cm^{-1})	−16
A(C–H)[a] (km mol^{-1})	18
Δr(C–F) (mÅ)	4.9
$\Delta\nu$(C–F) (cm^{-1})	−14, −17
R(CH···N) (Å)	2.30
ΔE (kcal mol^{-1})	−4.56
ΔE(CP)[b] (kcal mol^{-1})	−4.09
ΔE(CP + ZPE) (kcal mol^{-1})	−3.17

[a] A(C–H) of free CH_3F amounts to 22 km mol^{-1}.
[b] Counterpoise corrected.

$CHF_3\cdots NH_3$ can be treated as a conventional hydrogen-bonded complex, although the features that are usually invoked for such an assignment are comparatively weak.

We propose to explain of why $CHF_3\cdots OH_2$ and $CHF_3\cdots NH_3$ behave so differently in terms of selected scans for the intermolecular distances H···O and H···N, with all other geometrical parameters being subject to optimization. Since the structures **A**, **B** and **C** of $CHF_3\cdots OH_2$ are close in energy, the former scan is only performed for **A**. The resulting plots of R(C–H) as a function of R(H···O) for $CHF_3\cdots OH_2$ and that of R(H···N) for $CHF_3\cdots NH_3$ are displayed in Fig. 3. These plots demonstrate that, beginning from large intermolecular distances R(H···O) and R(H···N), R(C–H) gradually contracts, when the two molecules approach each other. In the case of $CHF_3\cdots OH_2$, R(C–H) contracts up to R(H···O) ~2.4 Å with the minimum close to 2.43 Å and is then lengthened again. At R(H···O) = 2.2 Å, close to the minimum value for **A**, the optimized R(C–H) = 1.0847 Å is still shorter than the equilibrium C–H bond length equal to 1.0856 Å of free CHF_3.

The case of $CHF_3\cdots NH_3$ is completely different: the minimum value of R(C–H) is achieved at R(H···N) of ca. 3 Å. At shorter R(H···N) distances, R(C–H) elongates. At the optimized R(H···N) ≈2.3 Å of the $CHF_3\cdots NH_3$ complex, R(C–H) is already larger than in free CHF_3. The origin of this behaviour is that the intermolecular interaction, due to the higher proton affinity of NH_3 as compared to H_2O, is slightly stronger for $CHF_3\cdots NH_3$. To rationalize this viewpoint, we perform a series of geometry optimizations (B3LYP/aug-cc-pVTZ) of CHF_3 in the presence of an external homogeneous electric dipole field chosen along the C–H bond. The corresponding results are displayed in Fig. 4. If the electric field is sufficiently small, R(C–H) undergoes a contraction. An increase of the field strength that mimics a stronger intermolecular

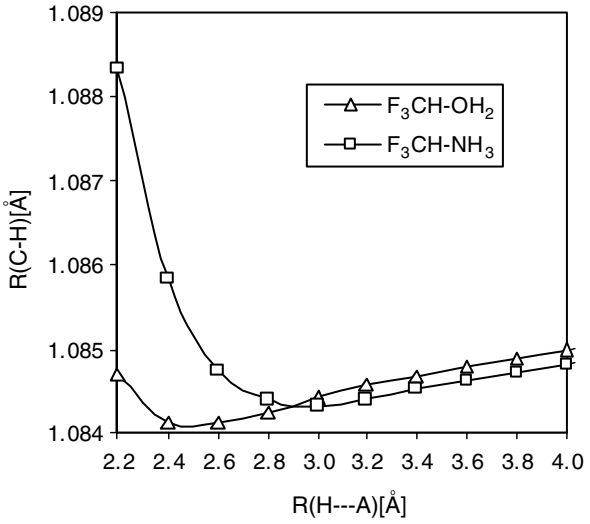

Fig. 3. The optimized R(C–H) bond length of CHF_3 upon scanning the intermolecular H···A distance in the $CHF_3\cdots OH_2$ and $CHF_3\cdots NH_3$ complexes (MP2/aug-cc-pVTZ).

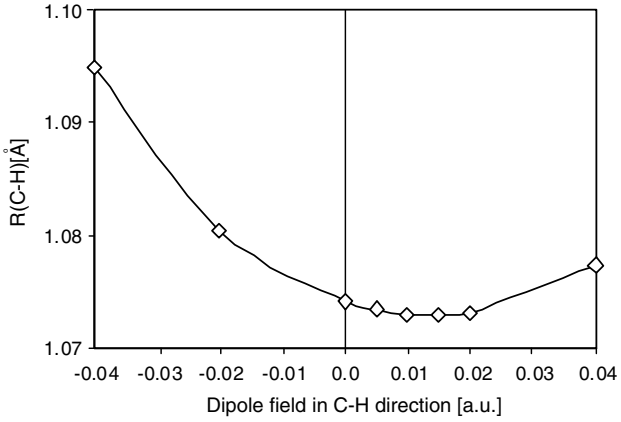

Fig. 4. The optimized R(C–H) distance of CHF_3 as a function of an electric dipole field in the direction of the C–H bond (B3LYP/aug-cc-pVTZ).

interaction reverses the trend and causes the C–H bond to elongate. In fact, all molecules that are considered as candidates for the blue-shifting effect are endowed with this type of response to an external homogeneous electric field: a contraction of R(X–H) at small field strengths, and an increase of R(X–H) at the larger. For fluoroform, this behaviour is a direct consequence of the specific INR feature of its *intramolecular energy surface*.

3. Theoretical ansatz: model Hamiltonian with linear mode coupling

In order to get insight into the origin of the intrinsic, intramolecular negative response of fluoromethanes, we propose a rather simple physical model mainly developed within the harmonic force field approach. Notice that the idea of applying the force field to blue-shifting hydrogen bonds has recently been explored by Qian and Krimm [19,35,36], and Karpfen and Kryachko [20].

To embark on with the model, let first note that each fluoromethane molecule CH_nF_{4-n} ($1 \leqslant n \leqslant 3$) possesses 9 independent degrees of freedom; 4 of them are the radial ones associated with the four existing bonds, either C–H or C–F. The remaining 5 degrees of freedom are related to the bond angles. According to Refs.[22,23], these angular degrees of freedom undergo sufficiently small changes under the interaction of CH_nF_{4-n} with $(HF)_{1\leqslant m\leqslant 4}$ and can therefore be neglected.

3.1. Model: harmonic approximation

Within the harmonic force field approach, the radial potential energy function of CH_nF_{4-n} in the vicinity of its equilibrium ground-state geometry casts as

$$U_n^{\mathrm{h}}(\{x_i^{(n)}\}_{i=1}^4) = \frac{1}{2}\sum_{i,j=1}^{4} \mathbf{k}_{ij}^{(n)} x_i^{(n)} x_j^{(n)}. \tag{1}$$

Here, the bond displacement $x_i^{(n)} \equiv r_i - r_{ie}$, r_{ie} is the equilibrium length of the ith bond and $(\{x_i^{(n)}\}_{i=1}^4)$ are ordered as follows: the former $x_1^{(n)},\ldots,x_n^{(n)}$ correspond to the C–H bonds, whereas $x_{n+1}^{(n)},\ldots,x_4^{(n)}$ to the C–F ones. $\mathbf{K}^{(n)} \equiv (\mathbf{k}_{ij}^{(n)})_{1\leqslant i,j\leqslant 4}$ is the non-singular force constant matrix of CH_nF_{4-n}. Its matrix elements evaluated within the MP2/aug-cc-pVTZ and MP2/6-311++G(2d,2p) methods are collected in Table 3.

Assume that the 'spectator' C–F_4 bond length $x_4^{(n)} = x_0^{(n)}$ is determined by the formation of the (C)$F_4\cdots$H–A halogen–hydrogen bond and plays a role of parameter. This converts $U_n^{\mathrm{h}}(\{x_i^{(n)}\}_{i=1}^4)$ to the reduced potential energy function

$$u_n^{\mathrm{h}}\left(\{x_i^{(n)}\}_{i=1}^3; x_0^{(n)}\right) = \frac{1}{2}\sum_{i,j=1}^{3} \mathbf{k}_{ij}^{(n)} x_i^{(n)} x_j^{(n)} + \frac{1}{2} x_0^{(n)} \sum_{i=1}^{3} \mathbf{k}_{ij}^{(n)} x_i^{(n)} x_j^{(n)} \tag{2}$$

which parametrically depends on $x_0^{(n)}$ (note that the constant term (1/2) $\mathbf{k}_{44}^{(n)}(x_0^{(n)})^2$ is removed in Eq. (2)). Let further suggest that the reduced potential energy function $u_n^{\mathrm{h}}(\{x_i^{(n)}\}_{i=1}^3; x_0^{(n)})$ has an extremum at $\{x_{i0}^{(n)}\}_{i=1}^3$. The latter, $x_{i0}^{(n)}$ ($1 \leqslant i \leqslant 3$), linearly depend on $x_0^{(n)}$ due to the chosen harmonic ansatz and obey the following system of linear algebraic equations:

$$\begin{aligned} \mathbf{k}_{11}x_{10} + \mathbf{k}_{12}x_{20} + \mathbf{k}_{13}x_{30} &= -\mathbf{k}_{14}x_0 \\ \mathbf{k}_{12}x_{10} + \mathbf{k}_{22}x_{20} + \mathbf{k}_{23}x_{30} &= -\mathbf{k}_{24}x_0 \\ \mathbf{k}_{13}x_{10} + \mathbf{k}_{23}x_{20} + \mathbf{k}_{33}x_{30} &= -\mathbf{k}_{34}x_0 \end{aligned} \tag{3}$$

(the superscript (n) is dropped out for simplicity). The solution of the system (3) is simply expressed as the ratios of the corresponding minors of $\mathbf{K}^{(n)}$ to $\Delta = \det\mathbf{K}^{(n)}$, viz.,

$$x_{i0} = -(\Delta_i/\Delta)x_0, \quad i = 1,2,3, \tag{4}$$

where Δ_i and Δ are

$$\Delta = \begin{vmatrix} k_{11} & k_{12} & k_{13} \\ k_{12} & k_{22} & k_{23} \\ k_{13} & k_{23} & k_{33} \end{vmatrix}, \quad \Delta_1 = \begin{vmatrix} k_{14} & k_{12} & k_{13} \\ k_{24} & k_{22} & k_{23} \\ k_{34} & k_{23} & k_{33} \end{vmatrix}, \quad \Delta_2 = \begin{vmatrix} k_{11} & k_{14} & k_{13} \\ k_{12} & k_{24} & k_{23} \\ k_{13} & k_{34} & k_{33} \end{vmatrix}, \quad \Delta_3 = \begin{vmatrix} k_{11} & k_{12} & k_{14} \\ k_{12} & k_{22} & k_{24} \\ k_{13} & k_{23} & k_{34} \end{vmatrix} \tag{4'}$$

and are equal for each fluoromethane to

$$\begin{aligned} n = 1 : \Delta &= (\mathbf{k}_{22} - \mathbf{k}_{23})[\mathbf{k}_{11}(\mathbf{k}_{22} + \mathbf{k}_{23}) - 2\mathbf{k}_{12}^2], \\ \Delta_1 &= \mathbf{k}_{12}(\mathbf{k}_{22} - \mathbf{k}_{23})^2, \\ \Delta_2 &= \Delta_3 = (\mathbf{k}_{22} - \mathbf{k}_{23})(\mathbf{k}_{11}\mathbf{k}_{23} - \mathbf{k}_{12}^2); \end{aligned} \tag{5a}$$

$$n = 2 : \Delta = (\mathbf{k}_{11} - \mathbf{k}_{12})[\mathbf{k}_{33}(\mathbf{k}_{11} + \mathbf{k}_{12}) - 2\mathbf{k}_{13}^2]$$
$$\Delta_1 = \Delta_2 = (\mathbf{k}_{11} - \mathbf{k}_{12})(\mathbf{k}_{33} - \mathbf{k}_{34})\mathbf{k}_{13},$$
$$\Delta_3 = (\mathbf{k}_{11} - \mathbf{k}_{12})[\mathbf{k}_{34}(\mathbf{k}_{11} + \mathbf{k}_{12}) - 2\mathbf{k}_{13}^2]; \quad (5b)$$
$$n = 3 : \Delta = (\mathbf{k}_{11} - \mathbf{k}_{12})[\mathbf{k}_{11}(\mathbf{k}_{11} + \mathbf{k}_{12}) - 2\mathbf{k}_{12}^2]$$
$$\Delta_1 = \Delta_2 = \Delta_3 = (\mathbf{k}_{11} - \mathbf{k}_{12})^2\mathbf{k}_{14}. \quad (5c)$$

Since the latter are tabulated in Table 5, we finally obtain

$$n = 1 : x_{10} = -0.024x_0, x_{20} = x_{30} = -0.117x_0; \quad (6a)$$
$$n = 2 : x_{10} = x_{20} = -0.032x_0, x_{30} = -0.130x_0; \quad (6b)$$
$$n = 3 : x_{10} = x_{20} = x_{30} = -0.036x_0. \quad (6c)$$

Taking into account that all intramolecular coupling force constants $\mathbf{k}_{ij}$ ($i \neq j$) are positive ($\forall \mathbf{k}_{ii} > 0$) and $\mathbf{k}_{ij}/\mathbf{k}_{nn} \ll 1$ (see Table 5), we readily arrive at

$$n = 1 : \Delta \approx \mathbf{k}_{11}\mathbf{k}_{22}^2, \quad \Delta_1 \approx \mathbf{k}_{12}\mathbf{k}_{22}^2, \quad \Delta_2 = \Delta_3 \approx \mathbf{k}_{11}\mathbf{k}_{22}\mathbf{k}_{23}; \quad (5a')$$
$$n = 2 : \Delta \approx \mathbf{k}_{11}^2\mathbf{k}_{33}, \quad \Delta_1 = \Delta_2 \approx \mathbf{k}_{11}\mathbf{k}_{33}\mathbf{k}_{13}, \quad \Delta_3 \approx \mathbf{k}_{11}^2\mathbf{k}_{34}; \quad (5b')$$
$$n = 3 : \Delta \approx \mathbf{k}_{11}^3, \quad \Delta_1 = \Delta_2 = \Delta_3 \approx \mathbf{k}_{11}^2\mathbf{k}_{14}. \quad (5c')$$

The latter formulas provide the approximate solutions of (6):

$$n = 1 : x_{10}/x_0 \approx -\mathbf{k}_{12}/\mathbf{k}_{11} \approx -0.031, x_{20}/x_0 = x_{30}/x_0 \approx -\mathbf{k}_{23}/\mathbf{k}_{22} \approx -0.134; \quad (6a')$$
$$n = 2 : x_{10}/x_0 = x_{20}/x_0 \approx -\mathbf{k}_{13}/\mathbf{k}_{11} \approx -0.037, x_{30}/x_0 \approx -\mathbf{k}_{34}/\mathbf{k}_{33} \approx -0.132; \quad (6b')$$
$$n = 3 : x_{10}/x_0 = x_{20}/x_0 = x_{30}/x_0 \approx -\mathbf{k}_{14}/\mathbf{k}_{11} \approx -0.036. \quad (6c')$$

Eqs. (6) and (6') demonstrate that all the ratios x_{i0}/x_0 ($i = 1 \div 3$) are negative. Therefore, all fluoromethanes feature a negative response, i.e., if a given spectator C–F_4 bond is stretched, each fluoromethane responds by shortening of all other C–H and C–F bonds, viz.,

$$r_i = r_{ie} - (\Delta_i/\Delta)(r_4 - r_{4e}), \quad (\Delta_i/\Delta) > 0 (i = 1 \div 3). \quad (7)$$

A trivial comparison of Eqs. (6a)–(6c) reveals that fluoroform is characterized by the largest negative response for its C–H bonds, whereas methylene fluoride features the largest negative response for its non-participating C–F bond. Since the esti-

Table 5
The harmonic force constants (mdyne Å^{-1}) of CH_nF_{4-n} ($1 \leqslant n \leqslant 3$) evaluated within the MP2/aug-cc-pVTZ and MP2/6-311++G(2d,2p) approaches using the GAR2PED program [37]

	CHF_3		CH_2F_2		CH_3F	
	MP2/aug-cc-pVTZ	MP2/6-311++G(2d,2p)	MP2/aug-cc-pVTZ	MP2/6-311++G(2d,2p)	MP2/aug-cc-pVTZ	MP2/6-311++G(2d,2p)
$\mathbf{k}_{11}$	5.621	5.693	5.502	5.571	5.491	5.540
	5.684[a]		5.745[a]		5.590[a]	
$\mathbf{k}_{12}$	0.177	0.176	0.039	0.040	0.031	0.035
	0.132[a]		0.021[a]		0.020[a]	
$\mathbf{k}_{22}$	6.474	6.283	5.502	5.571	5.491	5.540
	5.567[a]		5.587[a]		5.605[a]	
$\mathbf{k}_{23}$	0.865	0.857	0.203	0.202	0.031	0.035
	0.867[a]		0.169[a]		0.022[a]	
$\mathbf{k}_{13}$	0.865	0.857	0.203	0.202	0.031	0.035
	0.138[a]		−0.130[a]		0.020[a]	
$\mathbf{k}_{33}$	6.474	6.283	6.098	5.903	5.491	5.540
	6.702[a]		5.736[a]		5.605[a]	
$\mathbf{k}_{34}$	0.865	0.857	0.807	0.795	0.198	0.197
	0.885[a]		0.729[a]		0.147[a]	
$\mathbf{k}_{14}$	0.177	0.176	0.203	0.202	0.198	0.197
	0.137[a]		0.226[a]		0.136[a]	
$\mathbf{k}_{44}$	6.474	6.283	6.098	5.903	5.776	5.586
	6.746[a]		6.417[a]		5.164[a]	
Δ	231.060	220.220	184.141	182.743	165.634	170.014
Δ_1	5.380	5.182	5.868	5.707	5.905	5.970
Δ_2	27.109	26.305	5.868	5.707	5.905	5.970
Δ_3	27.109	26.305	23.980	24.219	5.905	5.970

[a] Results of the present work: the selected force constants of the optimized structures $CH_nF_{4-n}\cdots(HF)_2$ ($1 \leqslant n \leqslant 3$; Refs. [22,23]).

mations provided by Eq. (6') are rather close to the corresponding exact solutions Eq. (6) , we conclude that a negative response of the entire series of fluoromethanes to the stretched spectator C–F bond originates from a positivity of the intramolecular coupling force constants Eq. (6'): the larger is the intermolecular mode coupling (if $\forall \mathbf{k}_{ii} > 0$), the larger is the negative response, and the larger is the blue shift of the respective C–H stretch. To measure the response of CH_nF_{4-n}, let us define the so-called harmonic response factors $\alpha_{hi}^{(n)} \equiv \Delta_i^{(n)}/\Delta^{(n)}$. Evidently, the regime of the negative response takes place if $\forall \alpha_{hi}^{(n)} > 0$. Fig. 1 definitely validates the proposed harmonic force model in estimating the harmonic response factors of fluoromethanes. Within the range of $[-20, -100]$ (mÅ) of the spectator C–F_4 bond length which is even far beyond those reported in Tables 1 and 2, the calculated α_h(C–H) varies from 0.024 to 0.020 for CHF_3, from 0.034 to 0.029 for CH_2F_2, and from 0.044 to 0.037 for CH_3F. The latter fairly agree with those given by Eqs. (6a)–(6c): the maximal absolute relative deviation comprises of only 10–20% that can be related to neglecting the bond stretch–bond angle coupling as probably an important factor and anharmonic corrections as well (see Section 3.3).

3.2. Symmetry-adapted harmonic ansatz

Fluoromethanes possess certain point symmetries: C_{3v} for fluoroform CHF_3 and methyl fluoride CH_3F, and C_{2v} for methylene fluoride CH_2F_2. Imposing the appropriate point symmetry on the potential energy function U_n^h given by Eq. (1) entails the symmetry decouplings of its terms that converts U_n^h into the following symmetry-adapted potential energy function

$$U_{n\,\mathrm{sym}}^{h}(Q_1^{(n)}, Q_2^{(n)}) = \frac{1}{2}K_{11}^{(n)}[Q_1^{(n)}]^2 + \frac{1}{2}K_{22}^{(n)}[Q_2^{(n)}]^2 + K_{12}^{(n)}Q_1^{(n)}Q_2^{(n)}. \tag{8}$$

In Eq. (8),

$$Q_1^{(n)} = \frac{1}{\sqrt{n}}\sum_{i=1}^{n}(r_i - r_{ie}) \quad \text{and} \quad Q_2^{(n)} = \frac{1}{\sqrt{4-n}}\sum_{i=n+1}^{4}(r_i - r_{ie}) \tag{9}$$

are the symmetric bond displacements defined in Ref. [38] (see also Refs. [39,40] and references therein). The corresponding force constants $K_{11}^{(n)}$, $K_{22}^{(n)}$, and $K_{12}^{(n)}$ of fluoromethanes are tabulated in Table 6.

By a straightforward analogy with the previous subsection, we consider $Q_2^{(n)}$ as a parameter fixed at $Q_2^{(n)} = Q_{20}^{(n)}$. The extremum of $u_{n\,\mathrm{sym}}^{h}(Q_1^{(n)}; Q_{20}^{(n)})$ as a function of $Q_1^{(n)}$ taken at $Q_{20}^{(n)}$ is attained at $Q_{10}^{(n)}$ that satisfies the equation

$$K_{11}^{(n)}Q_{10}^{(n)} + K_{12}^{(n)}Q_{20}^{(n)} = 0. \tag{10}$$

Rewriting the latter as

$$\Sigma_{i=1}^{n}(r_i - r_{ie}) = -\sqrt{\frac{n}{4-n}}(K_{12}^{(n)}/K_{11}^{(n)})Q_{20}^{(n)} \tag{11}$$

allows to determine the minimum of $u_{n\,\mathrm{sym}}^{h}(Q_1^{(n)}; Q_{20}^{(n)})$,

$$u_{n\,\mathrm{sym}}^{h}(Q_{10}^{(n)}; Q_{20}^{(n)}) = \frac{1}{2}[K_{22}^{(n)} - (K_{12}^{(n)})^2/K_{11}^{(n)}](Q_{20}^{(n)})^2, \tag{12}$$

if $K_{22}^{(n)} > (K_{12}^{(n)})^2/K_{11}^{(n)}$. As directly follows from Table 6, the latter inequality holds for the entire fluoromethane series.

Eq. (11) implies that if $Q_{20}^{(n)} > 0$, i.e., all C–F bonds are simultaneously stretched, and the coupling force constant $K_{12}^{(n)} > 0$ ($K_{11}^{(n)} > 0$ due to stability of a given molecule), the C–H bonds are shortened. This determines the regime of a negative response. Positive $Q_{20}^{(n)}$ and $K_{12}^{(n)}$ settle the regime of a positive response. Taking the analogy with the preceding Subsection, it is worth therefore to introduce a symmetric harmonic response factor $\alpha_{sh}^{(n)} \equiv K_{12}^{(n)}/K_{11}^{(n)}$. Using Table 6, we obtain that $\alpha_{sh}^{(1)}(CHF_3) = 0.048 < \alpha_{sh}^{(3)}(CH_3F) = 0.068 < \alpha_{sh}^{(2)}(CH_2F_2) = 0.080$. Note also that $\alpha_{sh}^{(3)}(CH_3Cl) = 0.015$, as evaluated from $K_{11}^{(3)} = 5.755$ [42], 5.558 [43] mdyne Å^{-1}, $K_{12}^{(3)} = 0.086$ [42], 0.085 [43] mdyne Å^{-1}, and $K_{22}^{(3)} = 3.778$ [42], 3.597 [43] mdyne Å^{-1}, is smaller than the symmetric harmonic response factor of any fluoromethane.

Table 6
The symmetry-adapted force constants (mdyne Å^{-1}) of fluoromethanes

	CHF_3 [38]	CH_2F_2 [41]	CH_3F [42]
K_{11}	8.319	8.177	5.471
K_{12}	0.258	0.479	0.372
K_{22}	5.426	5.992	6.099

3.3. First-order anharmonic model

An inclusion of the first-order anharmonic corrections transforms the harmonic potential energy function $U^{\mathrm{h}}_{n\,\mathrm{sym}}(Q^{(n)}_1, Q^{(n)}_2)$ given by Eq. (8) into

$$U^{\mathrm{anh}}_{n\,\mathrm{sym}}(Q^{(n)}_1, Q^{(n)}_2) = U^{\mathrm{h}}_{n\,\mathrm{sym}}(Q^{(n)}_1, Q^{(n)}_2) + \frac{1}{6}(K^{(n)}_{111}[Q^{(n)}_1]^3 + K^{(n)}_{222}[Q^{(n)}_2]^3) + \frac{1}{3}(K^{(n)}_{112}[Q^{(n)}_1]^2 Q^{(n)}_2 + K^{(n)}_{122} Q^{(n)}_1 [Q^{(n)}_2]^2). \tag{13}$$

Given $Q^{(n)}_2 = Q^{(n)}_{20}$, $u^{\mathrm{anh}}_{n\,\mathrm{sym}}(Q^{(n)}_1; Q^{(n)}_{20})$ as a function of $Q^{(n)}_1$ reaches the extremum at $Q^{(n)}_{10}$ that obeys the quadratic algebraic equation

$$[Q^{(n)}_{10}]^2 + (2/K^{(n)}_{111})[K^{(n)}_{11} + \frac{2}{3}K^{(n)}_{122}Q^{(n)}_{20}]Q_1 + (2/K^{(n)}_{111})[K^{(n)}_{12} + \frac{1}{3}K^{(n)}_{122}Q^{(n)}_{20}]Q^{(n)}_{20} = 0. \tag{14}$$

The relevant root of Eq. (14) is expressed as

$$Q^{(n)}_{10} = -(1/K^{(n)}_{111})\left\{[K^{(n)}_{11} + \frac{2}{3}K^{(n)}_{112}Q^{(n)}_{20}] - [[K^{(n)}_{11}]^2 + \left(\frac{2}{3}K^{(n)}_{11}K^{(n)}_{112} - 2K^{(n)}_{12}K^{(n)}_{111}\right)Q^{(n)}_{20} + \left(\frac{4}{9}[K^{(n)}_{112}]^2 - \frac{2}{3}K^{(n)}_{122}K^{(n)}_{111}\right)[Q^{(n)}_{20}]^2]^{1/2}\right\}. \tag{15}$$

To the second order of $Q^{(n)}_{20}$, $Q^{(n)}_{10}$ can be approximated by

$$Q^{(n)[2]}_{10} = -[(K^{(n)}_{12}/K^{(n)}_{11}) + (K^{(n)}_{112}/3K^{(n)}_{111})]Q^{(n)}_{20} + (1/K^{(n)}_{11})[(2K^{(n)}_{12}K^{(n)}_{112}/K^{(n)}_{11}) - K^{(n)}_{111}[K^{(n)}_{12}/K^{(n)}_{11}]^2 + ([K^{(n)}_{122}]^2/9K^{(n)}_{111}) - \frac{1}{3}K^{(n)}_{122}][Q^{(n)}_{20}]^2. \tag{16}$$

Assume that the first term in the square brackets on the r.h.s. of Eq. (16) is the leading. Then, this equation determines a negative response if $\alpha^{(n)}_{\mathrm{anh}} \equiv (K^{(n)}_{12}/K^{(n)}_{11}) + (K^{(n)}_{112}/3K^{(n)}_{111})$ is positive, and a positive one otherwise. The anharmonic response factors $\alpha^{(n)}_{\mathrm{anh}}$ of fluoromethanes are equal to 0.043 (CHF_3: $K^{(1)}_{111} = -46.844$ mdyne Å^{-2} and $K^{(1)}_{112} = -1.673$ mdyne Å^{-2} [38]), 0.074 (CH_2F_2; $K^{(2)}_{111} = -43.486$ mdyne Å^{-2} and $K^{(2)}_{112} = -2.673$ mdyne Å^{-2} [41]), and to 0.064 (CH_3F: $K^{(3)}_{111} = -18.101$ [41], -17.18 [44], -19.222 [45] mdyne Å^{-2} and $K^{(3)}_{112} = 0.201$ [43], 0.20 [44], 0.235 [45] mdyne Å^{-2}). A comparison of these values of $\alpha^{(n)}_{\mathrm{anh}}$ with $\alpha^{(n)}_{\mathrm{h}}$ shows that the corresponding contribution of the first-order anharmonic corrections comprises of ca. 10%, 7%, and 5%, and can therefore be neglected (note also that the anharmonic contribution to $\alpha^{(3)}_{\mathrm{anh}}$ is negative, whereas it is positive for CHF_3 and CH_2F_2).

3.4. Harmonic model: lifting a symmetry

A deviation of a single spectator C–F_4 bond of the CH_2F_2 and CHF_3 molecules from the equilibrium as a result of the formation of the conventional hydrogen bond (C)$F_4\cdots$H–B obviously breaks their point symmetries (see Tables 1 and 2). The appropriate description of this point-symmetry breaking relies on the total potential energy of a given fluoromethane that should necessarily include all its normal radial displacements. Consider the CHF_3 molecule as a key example. The total potential energy function of $CHF_3$is represented by

$$U^{\mathrm{h}}_{\mathrm{CHF_3}}(\{Q_k\}_{1\leqslant k\leqslant 4}) = \frac{1}{2}[K_{11}Q_1^2 + K_{22}Q_2^2 + K_{33}Q_3^2 + K_{44}Q_4^2] + K_{12}Q_1Q_2, \tag{17}$$

where $Q_1 = r_1 - r_{1\mathrm{e}}$, $Q_2 = \frac{1}{\sqrt{3}}\sum_{i=2}^{4}(r_i - r_{i\mathrm{e}})$, $Q_3 = \frac{1}{\sqrt{6}}[2(r_2 - r_{2\mathrm{e}}) - (r_3 - r_{3\mathrm{e}}) - (r_4 - r_{4\mathrm{e}})]$, and $Q_4 = \frac{1}{\sqrt{2}}[(r_3 - r_{3\mathrm{e}}) - (r_4 - r_{4\mathrm{e}})]$ are the normal displacements. Introducing the C–F bond displacements of CHF_3 as $q_k = r_k - r_{k\mathrm{e}}$ $(2 \leqslant k \leqslant 4)$, suggesting that the last one is fixed at $q_4 \equiv q_{40}$, and finally recollecting terms in Eq. (17), we arrive at

$$\begin{aligned} u^{\mathrm{h}}_{\mathrm{CHF_3}}(Q_1, \{q_k\}_{2\leqslant k\leqslant 3}; q_{40}) = {} & \frac{1}{2}K_{11}Q_1^2 + \frac{1}{6}(K_{22} + 2K_{33})q_2^2 + \frac{1}{12}(2K_{22} + K_{33} + 3K_{44})q_3^2 + K_{12}Q_1(q_2 + q_3 + q_{40}) \\ & + \frac{1}{3}(K_{22} - K_{33})(q_2q_3 + q_2q_{40}) + \frac{1}{6}(2K_{22} + K_{33})q_3q_{40} + \frac{1}{12}(2K_{22} + K_{33} + 3K_{44})q_{40}^2. \end{aligned} \tag{18}$$

Taking sequentially the first derivatives of $u^{\mathrm{h}}_{\mathrm{CHF_3}}(Q_1, \{q_k\}_{1\leqslant k\leqslant 4}; q_{40})$ with respect to all involved variables and equating them to zero, we obtain the system of linear algebraic equations

$$\begin{aligned} & K_{11}Q_1 + K_{12}(q_2 + q_3 + q_{40}) = 0 \\ & K_{12}Q_1 + \kappa_{22}q_2 + \kappa_{23}(q_3 + q_{40}) = 0 \\ & K_{12}Q_1 + \kappa_{23}q_2 + \kappa_{33}q_3 + \kappa_{34}q_{40} = 0, \end{aligned} \tag{19}$$

with the modified force constants $\kappa_{22} = \frac{1}{3}(K_{22} + 2K_{33})$, $\kappa_{23} = \frac{1}{3}(K_{22} - K_{33})$, $\kappa_{33} = \frac{1}{12}(2K_{22} + K_{33} + 3K_{44})$, and $\kappa_{34} = \frac{1}{6}(2K_{22} + K_{33})$. The solution of the system (19) then reads as

$$Q_{10} = -(\Delta_1/\Delta)q_{40}, q_{20} = -(\Delta_2/\Delta)q_{40}, \quad \text{and } q_{30} = -(\Delta_3/\Delta)q_{40},$$

where

$$\Delta = \frac{1}{3}K_{11}[\frac{1}{6}K_{22}K_{33} + \frac{1}{2}K_{22}K_{44} + K_{33}K_{44}] - \frac{1}{2}K_{12}^2(3K_{33} + K_{44}), \quad \Delta_1 = \frac{1}{2\sqrt{3}}K_{12}K_{33}K_{44},$$
$$\Delta_2 = \frac{1}{6}K_{44}[K_{11}(K_{22} - K_{33}) - K_{12}^2], \quad \Delta_3 = \frac{1}{2}K_{33}(K_{11}K_{22} - K_{12}^2). \tag{20}$$

The CH_2F_2 molecule can be considered in a similar fashion, namely, we first define its potential energy function,

$$U^{\mathrm{h}}_{CH_2F_2}(\{Q_k\}_{1\leqslant k\leqslant 4}) = \frac{1}{2}[K_{11}Q_1^2 + K_{22}Q_2^2 + K_{33}Q_3^2 + K_{44}Q_4^2] + K_{12}Q_1Q_2 + K_{34}Q_3Q_4, \tag{21}$$

in terms of the normal displacements $Q_1 = \frac{1}{\sqrt{2}}\sum_{i=1}^{2}(r_i - r_{ie})$, $Q_2 = \frac{1}{\sqrt{2}}\sum_{i=3}^{4}(r_i - r_{ie})$, $Q_3 = \frac{1}{\sqrt{2}}[(r_1 - r_{1e}) - (r_2 - r_{2e})]$, $Q_4 = \frac{1}{\sqrt{2}}[(r_3 - r_{3e}) - (r_4 - r_{4e})]$. Then introduce sequentially the C–H and C–F bond displacements as $q_k = r_k - r_{ke}$ ($1 \leqslant k \leqslant 4$) and hold the last one at $q_4 \equiv q_{40}$. This transforms $U^{\mathrm{h}}_{CH_2F_2}(\{Q_k\}_{1\leqslant k\leqslant 4})$ into the reduced potential energy function

$$u^{\mathrm{h}}_{CH_2F_2}(\{q_k\}_{1\leqslant k\leqslant 3}; q_{40}) = \frac{1}{4}(K_{11} + K_{33})(q_1^2 + q_2^2) + \frac{1}{2}(K_{11} - K_{33})q_1q_2 + \frac{1}{4}(K_{22} + K_{44})(q_3^2 + q_{40}^2) + \frac{1}{2}(K_{22} - K_{44})q_3q_{40}$$
$$+ \frac{1}{2}(K_{12} + K_{34})(q_1q_3 + q_2q_{40}) + \frac{1}{2}(K_{12} - K_{34})(q_1q_{40} + q_2q_3). \tag{22}$$

Equating the first derivatives of $u^{\mathrm{h}}_{CH_2F_2}$ with respect to $q_{1\leqslant k\leqslant 3}$ to zero yields the following system of linear algebraic equations:

$$\begin{aligned}
&(K_{11} + K_{33})q_1 + (K_{11} - K_{33})q_2 + (K_{22} + K_{44})q_3 = -(K_{12} - K_{34})q_{40},\\
&(K_{11} - K_{33})q_1 + (K_{11} + K_{33})q_2 + (K_{12} - K_{34})q_3 = -(K_{12} + K_{34})q_{40},\\
&(K_{12} + K_{34})q_1 + (K_{12} - K_{34})q_2 + (K_{22} + K_{44})q_3 = -(K_{22} - K_{44})q_{40}.
\end{aligned} \tag{23}$$

The solutions of (23) are expressed as $q_{k0} = -(\Delta_k/\Delta)q_{40}$ ($1 \leqslant k \leqslant 3$), where

$$\Delta = \frac{1}{2}[K_{11}K_{33}(K_{22} + K_{44}) + K_{11}K_{12}^2 + K_{33}K_{34}^2], \quad \Delta_1 = \frac{1}{2}[(K_{12}K_{33}K_{44} - K_{11}K_{22}K_{34}) + (K_{12} - K_{34})K_{12}K_{34}],$$
$$\Delta_2 = \frac{1}{2}[(K_{12}K_{33}K_{44} - K_{11}K_{22}K_{34}) - (K_{12} + K_{34})K_{12}K_{34}],$$
$$\Delta_3 = \frac{1}{4}[2(K_{22} - K_{44})K_{11}K_{33} + 2(K_{11} - K_{33})K_{12}K_{34} - (K_{11} + K_{33})(K_{12}^2 - K_{34}^2)]. \tag{24}$$

4. Effect of external field

Within the harmonic force field model introduced in Section 3.1, the radial potential energy function of the fluoromethane CH_nF_{4-n} embedded into an external inhomogeneous electric field $\mathbf{E}$ is approximated by (see, e.g., Ref. [46])

$$U^{\mathrm{h}}_n(\{x_i^{(n)}\}_{i=1}^4;\ \mathbf{E}) = \frac{1}{2}\sum_{i,j=1}^{4}\mathbf{k}_{ij}^{(n)}x_i^{(n)}x_j^{(n)} + \sum_{i=1}^{4}\mathbf{E}_i(\partial\boldsymbol{\mu}/\partial x_i^{(n)})x_i^{(n)}, \tag{25}$$

where $\boldsymbol{\mu}$ is the total dipole moment and $\mathbf{E}_i$ is the strength of the electric field at the C–H_i (if $1 \leqslant i \leqslant n$) or C–$F_i$ (if $n + 1 \leqslant i \leqslant 4$) bond. Assuming that the 'spectator' C–F_4 bond is a parameter, x_0, which is determined by the C–$F_4\cdots$H–A hydrogen bond that CH_nF_{4-n} is formed with the proton-donor molecule A–H and which also accounts the change produced by an external electric field, we write the system of linear algebraic equations that defines the equilibrium geometry:

$$\begin{aligned}
&\mathbf{k}_{11}x_{10} + \mathbf{k}_{12}x_{20} + \mathbf{k}_{13}x_{30} = -\mathbf{k}_{14}x_0 - \mathbf{E}_1\partial\boldsymbol{\mu}/\partial x_1\\
&\mathbf{k}_{12}x_{10} + \mathbf{k}_{22}x_{20} + \mathbf{k}_{23}x_{30} = -\mathbf{k}_{24}x_0 - \mathbf{E}_2\partial\boldsymbol{\mu}/\partial x_2\\
&\mathbf{k}_{13}x_{10} + \mathbf{k}_{23}x_{20} + \mathbf{k}_{33}x_{30} = -\mathbf{k}_{34}x_0 - \mathbf{E}_3\partial\boldsymbol{\mu}/\partial x_3.
\end{aligned} \tag{26}$$

The solution of the system (26) is obviously expressed as

$$x_{io}(\mathbf{E}) = -\Delta_i(\mathbf{E})/\Delta, \tag{27}$$

where $\Delta_i(\mathbf{E})$ and Δ are determined by Eq. (4′) with replacing $\mathbf{k}_{i4}$ by $\mathbf{k}_{i4}x_0 + \mathbf{E}_i\partial\boldsymbol{\mu}/\partial x_i$. The former three minors can be explicitly represented as

$$\Delta_i(\mathbf{E}) = \Delta_i(0)x_0 + (-1)^{i-1}[\delta_1\Delta_{14}^{(i)} - \delta_2\Delta_{24}^{(i)} + \delta_3\Delta_{34}^{(i)}], \tag{28}$$

Table 7
The bond dipole moment derivatives (D/Å a.m.u.) of CH_nF_{4-n} ($1 \leqslant n \leqslant 3$) calculated at the MP2/aug-cc-pVTZ and MP2/6-311++G(2d,2p) computational levels using the GAR2PED program [37]

Bond	CHF_3		CH_2F_2		CH_3F	
	MP2/aug-cc-pVTZ	MP2/6-311++G(2d,2p)	MP2/aug-cc-pVTZ	MP2/6-311++G(2d,2p)	MP2/aug-cc-pVTZ	MP2/6-311++G(2d,2p)
$C–X_1$	0.018	−0.452	0.0	0.0	0.404	0.377
	−0.528	−0.265	0.0	0.0	0.027	−0.152
	0.0	0.0	−0.771	−0.775	0.0	0.0
$C–X_2$	0.528	−0.265	0.0	0.0	−0.027	0.152
	0.018	0.452	−5.475	5.529	0.404	0.377
	0.0	0.0	0.0	0.0	0.0	0.0
$C–X_3$	0.0	0.0	0.0	0.0	0.0	0.0
	0.0	0.0	0.0	0.0	0.0	0.0
	1.240	1.237	3.402	−3.462	−0.399	−0.509
$C–X_4$	0.0	0.0	1.388	1.420	0.0	0.0
	0.0	0.0	0.0	0.0	0.0	0.0
	3.332	−3.421	0.0	0.0	−3.543	−3.534

The Cartesian x, y, and z components are displayed from top to the bottom. X = H, F. The bond convention is defined in Section 3.1.

where $\delta_m = \mathbf{E}_m \partial \boldsymbol{\mu}/\partial x_m$ (the dipole moment derivatives are presented in Table 7). $\Delta_{14}^{(i)}$, $\Delta_{24}^{(i)}$, and $\Delta_{34}^{(i)}$ are the cofactors of $\mathbf{k}_{14}$, $\mathbf{k}_{24}$, and $\mathbf{k}_{34}$, respectively, of the matrix Δ_i. $\Delta_i(0)$ are given by Eqs. (5a)–(5c). Eq. (27) with $i = 1$ determines the displacement $x_{1o}(\mathbf{E})$ of the $C–H_1$ bond equal to:

$$CHF_3 : x_{1o}(\mathbf{E}) \approx -0.024x_o + 0.178\mathbf{E}_1 \partial \boldsymbol{\mu}/\partial x_1 - 0.024\mathbf{E}_3 \partial \boldsymbol{\mu}/\partial x_3 \quad (29a)$$

$$CH_2F_2 : x_{1o}(\mathbf{E}) \approx -0.032x_o + 0.182\mathbf{E}_1 \partial \boldsymbol{\mu}/\partial x_1 - 0.006\mathbf{E}_3 \partial \boldsymbol{\mu}/\partial x_3 \quad (29b)$$

$$CH_3F : x_{1o}(\mathbf{E}) \approx -0.036x_o + 0.182\mathbf{E}_1 \partial \boldsymbol{\mu}/\partial x_1. \quad (29c)$$

Assuming the homogeneous external electric field, we readily obtain from Eqs. (29a)–(29c) that

$$CHF_3 : x_{1o}(\mathbf{E}) \approx -0.024x_o - 0.121E, \quad (30a)$$

$$CH_2F_2 : x_{1o}(\mathbf{E}) \approx -0.032x_o - 0.160E, \quad (30b)$$

$$CH_3F : x_{1o}(\mathbf{E}) \approx -0.036x_o + 0.078E. \quad (30c)$$

Eq. (30a)–(30c) suggest the following picture of how an external electric field $\mathbf{E}$ affects the INR feature of fluoromethanes: if $\mathbf{E}$ and $\boldsymbol{\mu}$ are parallel, the homogeneous electric field strengthens the negative response regime of CHF_3 and CH_2F_2 and weakens it for CH_3F whose zeroth response regime is determined by the threshold value $E_{thr}(CH_3F) \approx 0.46$ x_o. In the opposite case, the external field lowers the negative harmonic response factor of CH_3F and increases those of CHF_3 and CH_2F_2. For the latter fluoromethanes, $E_{thr}(CHF_3) \approx E_{thr}(CH_2F_2) \approx 0.20x_o$. We may notice that E_{thr} of CH_3F is larger compared to those of other fluoromethanes, i.e., methyl fluoride is more reluctant to hold its intrinsic negative regime under stronger external homogeneous electric fields oriented parallel to its total dipole moment.

5. Summary and conclusions

In the present work, we have demonstrated that the contraction of the C–H bonds of fluoromethanes in some subclass of blue-shifting complexes and the concomitant blue shifts of their stretching vibrational modes originate from the elongation of the 'spectator' C–F bond that the latter experiences while forming the leading C–F···H–Y halogen–hydrogen bond with a conventional proton-donor molecule Y–H. It is therefore an intrinsic, intramolecular feature endowed by the entire series of fluoromethanes that underlies the phenomenon of an 'intrinsic, intramolecular negative response'. Therefore, the following picture of the key mechanism of the blue shift for the subclass of the so-called blue-shifted complexes emerges:

Suppose that a given INR 'host' molecule contains a X–A bond that is prone to behave as a proton acceptor and X–H bonds, and suppose that it interacts with a conventional proton-donor 'guest' molecule Y–H via forming a presumably dominant halogen–hydrogen bond X–A···H–Y, where an INR molecule acts as proton acceptor through its X–A bond, and thus attaining the global energetic minimum on their potential energy surface. Since the X–H bonds of the studied INR molecule possess, by definition, the INR property with respect to a vicinal, the so-called 'spectator' X–A bond, the X–A···H–Y halogen–hydrogen bond causes them to contract and thus to shift their X–H stretching vibrational modes to higher wavenumbers. Let us, moreover, suggest that at least one of the X–H bonds is involved in the auxiliary X–H···guest H-bond-type contact. Two scenarios are then possible: either this X–H bond elongates as a conventional proton-donor

bond or shortens as a hypothetical non-conventional one. The net effect in the latter scenario is a further contraction and a larger concomitant blue shift. The former scenario leads to a less contracted X–H bond since, as suggested, the X–A···H–Y hydrogen bonding interaction is leading and, therefore, it contracts the X–H bond stronger, as compared to the elongation produced by the auxiliary X–H···guest H-bond-type contact.

To understand the mechanism of the intrinsic, intramolecular negative response of fluoromethanes, we have proposed a simple physical and analytically solvable model which is largely based on the harmonic force field. We have explicitly shown that this model is in a good agreement with the calculated data on the contraction of the C–H bonds in the fluoromethanes–hydrogen fluoride complexes $CH_nF_{4-n}\cdots(HF)_{1\leqslant m\leqslant 4}$ ($1\leqslant n\leqslant 3$). Moreover, this model allows us to conclude that it is actually the intramolecular mode coupling pattern of fluoromethanes that entail the intrinsic negative response. Moreover, it allows to predict, by analogy with the recent work [20], new molecules as candidates for forming blue-shifted complexes.

Finally, we have revisited the rather enigmatic nature of the formation of the complexes $CHF_3\cdots OH_2$ and $CHF_3\cdots NH_3$ that, as we believe, unequivocally demonstrates a multi-facet phenomena of blue-shifting that cannot be entirely explained in terms of the intrinsic negative response and the intramolecular coupling patterns alone. In that case, one has also to consider that with increasing strength of the intermolecular interaction, approximately equivalent to a stronger electric field, the weak-field response of the fluoromethane is qualitatively changed (see again Fig. 4) in a way reminiscent to classical, conventional hydrogen bonding. In general, for large intermolecular interactions complexes with molecules that show the INR response for weaker fields, and hence display blue shifts, will have the properties similar to conventional red-shifted hydrogen-bonded complexes again. However, for the class of the cyclic fluoromethane–hydrogen fluoride complexes $CH_nF_{4-n}\cdots(HF)_{1\leqslant m\leqslant 4}$ ($1\leqslant n\leqslant 3$) analyzed in this work, this intrinsic behavior of the fluoromethanes appears to underlie the basic mechanism that causes their stability and the existence of strongly blue-shifted C–H···F hydrogen bonds.

Acknowledgements

We faithfully dedicate our work in the honour of Professor Lenz Cederbaum on the occasion of his 60th birthday. One of us, E.S.K., wholeheartedly appreciates Lenz for his permanent and kindest supports, and inspiring and stimulating discussions.

One of the authors, E.S.K., gratefully thanks Profs. Camille Sandorfy and Austin Barnes for the encouraging discussions and useful suggestions, and Francoise Remacle for warm hospitality. This work (E.S.K.) was partially supported by the EC FET-OPEN STREP Project MOLDYNLOGIC. The calculations were performed on the Linux-cluster Schrödinger III at the University of Vienna. We also thank the reviewer for valuable comments and suggestions.

References

[1] P. Hobza, Z. Havlas, Chem. Rev. 100 (2000) 4253.
[2] A.J. Barnes, J. Mol. Struct. 704 (2004) 3, and references therein.
[3] S.J. Grabowski (Ed.), Hydrogen Bonding – New Insights, Springer, Dordrecht, 2006, and references therein.
[4] C.G. Pimentel, A.L. McClellan, The Hydrogen Bond, Freeman, San Francisco, 1960;
, See also:G.C. Pimentel, A.L. McClellan, Annu. Rev. Phys. Chem. 22 (1971) 347.
[5] P. Schuster, G. Zundel, C. Sandorfy (Eds.), The Hydrogen Bond. Recent Developments in Theory and Experiments, North-Holland, Amsterdam, 1976.
[6] G.A. Jeffrey, W. Saenger, Hydrogen Bonding in Biological Structures, second ed., Springer, Berlin, 1994.
[7] G.A. Jeffrey, An Introduction to Hydrogen Bonding, Oxford University Press, Oxford, 1997.
[8] S. Scheiner, Hydrogen Bonding. A Theoretical Perspective, Oxford University Press, Oxford, 1997.
[9] G.R. Desiraju, T. Steiner, The Weak Hydrogen Bond in Structural Chemistry and Biology, Oxford University Press, Oxford, 1999;
, See also:G.R. Desiraju, Acc. Chem. Res. 29 (1996) 441;
G.R. Desiraju, Chem. Commun. (2005) 2995.
[10] T. Steiner, Angew. Chem., Int. Ed. 41 (2002) 48.
[11] Y. Gu, T. Kar, S. Scheiner, J. Am. Chem. Soc. 121 (1999) 9411.
[12] P. Hobza, Z. Havlas, Chem. Phys. Lett. 303 (1999) 447.
[13] E.S. Kryachko, T. Zeegers-Huyskens, J. Phys. Chem. A 105 (2001) 7118.
[14] I.V. Alabugin, M. Manoharan, S. Peabody, F. Weinhold, J. Am. Chem. Soc. 125 (2003) 5973.
[15] L. Pejov, K. Hermansson, J. Chem. Phys. 119 (2003) 313.
[16] X. Li, L. Liu, H.B. Schlegel, J. Am. Chem. Soc. 124 (2002) 9639.
[17] A. Masunov, J.J. Dannenberg, R.H. Contreras, J. Phys. Chem. A 105 (2001) 4737.
[18] K. Hermansson, J. Phys. Chem. A 106 (2002) 4695.
[19] W. Qian, S. Krimm, J. Phys. Chem. A 106 (2002) 6628.
[20] A. Karpfen, E.S. Kryachko, J. Phys. Chem. A 109 (2005) 8930.
[21] A. Karpfen, J. Mol. Struct. (Theochem) 757 (2005) 203.
[22] A. Karpfen, E.S. Kryachko, Chem. Phys. 310 (2005) 77.
[23] A. Karpfen, E.S. Kryachko, J. Phys. Chem. A 107 (2003) 9724.

[24] A. Karpfen, J. Mol. Struct. (Theochem) 710 (2004) 85.
[25] S.L. Paulson, A.J. Barnes, J. Mol. Struct. 80 (1982) 151;
See also: S.L. Paulson, Ph. D. Thesis, University of Salford, 1984.
[26] I. Alkorta, S. Maluendes, J. Phys. Chem. 99 (1995) 6457.
[27] S. Scheiner, T. Kar, J. Phys. Chem. A 106 (2002) 1784.
[28] P. Hobza, Z. Havlas, Theor. Chem. Acc. 108 (2002) 325.
[29] W. Zierkiewicz, D. Michalska, Z. Havlas, P. Hobza, ChemPhysChem 3 (2002) 511.
[30] S.K. Rhee, S.H. Kim, S. Lee, J.Y. Lee, Chem. Phys. 297 (2004) 21.
[31] W. Zierkiewicz, P. Jurečka, P. Hobza, ChemPhysChem 6 (2005) 609.
[32] A. Kaldor, I.M. Mills, Spectrochim. Acta A 20 (1964) 523.
[33] M.J. Frisch, G.W. Trucks, H.B. Schlegel, G.E. Scuseria, M.A. Robb, J.R. Cheeseman, J.A. Montgomery Jr., T. Vreven, K.N. Kudin, J.C. Burant, J.M. Millam, S.S. Iyengar, J. Tomasi, V. Barone, B. Mennucci, M. Cossi, G. Scalmani, N. Rega, G.A. Petersson, H. Nakatsuji, M. Hada, M. Ehara, K. Toyota, R. Fukuda, J. Hasegawa, M. Ishida, T. Nakajima, Y. Honda, O. Kitao, H. Nakai, M. Klene, X. Li, J.E. Knox, H.P. Hratchian, J.B. Cross, C. Adamo, J. Jaramillo, R. Gomperts, R.E. Stratmann, O. Yazyev, A.J. Austin, R. Cammi, C. Pomelli, J.W. Ochterski, P.Y. Ayala, K. Morokuma, G.A. Voth, P. Salvador, J.J. Dannenberg, V.G. Zakrzewski, S. Dapprich, A.D. Daniels, M.C. Strain, O. Farkas, D.K. Malick, A.D. Rabuck, K. Raghavachari, J.B. Foresman, J.V. Ortiz, Q. Cui, A.G. Baboul, S. Clifford, J. Cioslowski, B.B. Stefanov, G. Liu, A. Liashenko, P. Piskorz, I. Komaromi, R.L. Martin, D.J. Fox, T. Keith, M.A. Al-Laham, C.Y. Peng, A. Nanayakkara, M. Challacombe, P.M.W. Gill, B. Johnson, W. Chen, M.W. Wong, C. Gonzalez, J.A. Pople, GAUSSIAN 03 (Revision A.1), Gaussian Inc., Pittsburgh, PA, 2003.
[34] S.M. Melikova, K.S. Rutkowski, P. Rodziewicz, A. Koll, Chem. Phys. Lett. 352 (2002) 301.
[35] W. Qian, S. Krimm, J. Phys. Chem. A 106 (2002) 11663.
[36] W. Qian, S. Krimm, J. Phys. Chem. A 109 (2005) 5608.
[37] J.M.L. Martin, C. Van Alsenoy, GAR2PED Program, University of Antwerp, Antwerpen, 1995.
[38] W.T. King, I.M. Mills, B. Crawford, J. Chem. Phys. 27 (1957) 455.
[39] G. Klatt, A. Willets, N.C. Handy, R. Tarroni, P. Palmieri, J. Mol. Spectrosc. 176 (1996) 64.
[40] D. Papoušek, Z. Papouškova, D.P. Chong, J. Phys. Chem. 99 (1995) 15387.
[41] J.F. Gaw, N.C. Handy, P. Palmieri, A.D. Esposti, J. Chem. Phys. 89 (1988) 959.
[42] S. Kondo, Y. Koga, T. Nakanaga, J. Chem. Phys. 81 (1984) 1951.
[43] G.M. Black, M.M. Law, J. Mol. Spectrosc. 205 (2001) 280.
[44] I.A. Atkinson, M.M. Law, Spectrochim. Acta Part A 58 (2002) 873.
[45] W. Schneider, W. Thiel, Chem. Phys. 159 (1992) 46.
[46] A.J. Stone, The Theory of Intermolecular Forces, Clarendon Press, Oxford, 1996.